Journal of Materials Chemistry

Cite this: J. Mater. Chem., 2012, 22, 6327

www.rsc.org/materials

PAPER

Tuning the surface chemistry of iPDMS for improved protein microarray performance†

Xing Liu,[aef] Yuanzi Wu,[b] Ya Gao,[c] Jie Wang,[a] Zhong Li,[a] Jun Han,[d] Gang Jin[e] and Hongwei Ma*[a]

Received 13th December 2011, Accepted 8th February 2012
DOI: 10.1039/c2jm16572d

Protein microarrays meet the need for large-scale, low cost and accurate assays in the post-genomic era. Efforts in revealing the internal relationship between surface chemistry and microarray quality may greatly help the realization of widespread protein microarray use. In this paper, we prepared iPDMS with various surface properties, which were studied in combination with other parameters such as [protein], spot size and environment conditions to identify the causes of array defects (exosmosis, coffee ring and overflow) and corresponding strategies to avoid them. Through this research, we determined that the optimal parameters and conditions of protein microarray fabrication for an iPDMS sheet were 50° < contact angle < 90°: array volume ≤10 nL, [capture antibody] at 50 μg mL^{-1}, fixed at 25 °C, and 60% humidity. We also identified some characteristics of protein microarray fabrication that may benefit other solid supporting materials (SSM) and serve as a good model of proteins interacting with various bio-interfaces.

Introduction

Protein microarrays have proven to be a powerful tool in many fields including proteomics, drug discovery and disease diagnosis.[1–15] It allows for massive parallel analyses, while requiring only picogram analyte consumption; these characteristics perfectly meet the emerging large-scale, low cost and accurate assay needs of the post-genomic era.[16] The development of a protein microarray depends on the advancement of three key elements, namely, the number of proteins to be printed, the performance of solid supporting materials (SSM), and the detection method. The development of protein engineering provides thousands of proteins to be printed.[17–21] In addition, the development of signal amplification methods[22–25] continuously enhances the sensitivity of protein microarrays, meeting more and more challenging needs. Great efforts were also devoted to the SSM field.[26–30] In addition to the development of new SSM, the research community should also emphasize the importance of the internal relationship between SSM surface chemistry and microarray fabrication.[31,32]

For protein microarrays, the SSM provides an appropriate environment to maintain the stable and active conformation of the captured proteins. The SSM is exposed to various protein solutions and reagents throughout the microarray assay process. This procedure requires the SSM to be not only robust and easy to operate, but also to avoid nonspecific protein adsorption (NPA). For example, nitrocellulose (NC) films, like paper, are very fragile and prone to leak-induced-cross contamination and are therefore difficult to handle. We recently reported a novel SSM,[33] namely, polymer coated initiator integrated poly(-dimethysiloxane) (iPDMS), which, as a silicon rubber, is elastic and easy to handle. While both glass slides and NC films need a blocking step to reduce NPA, we demonstrated that the polymer coated iPDMS had an outstanding capacity for preventing NPA.

It has come to our attention that the details of protein microarray fabrication are largely missing. For example, very little research has focused on the impact of chemical/physical properties of SSM on the interaction between the SSM and proteins.[31–35] This is because protein microarrays are viewed as arrayed ELISAs (abbreviation of Enzyme-Linked Immuno Sorbent Assay), and the fabrication of ELISAs is well developed. In traditional ELISAs, 100–200 μL of protein solution was placed into each well of micro-well plates (typically 96 well plates) and proteins were allowed to physically absorb on the 2D surface of the plate. Most fabrication defects that arose from liquid–SSM interactions could be ignored under such large quantities of protein consumption. Furthermore, except

[a]Division of Nanobiomedicine, Suzhou Institute of Nano-Tech and Nano-Bionics, Chinese Academy of Sciences, Suzhou, 215123, China. E-mail: hwma2008@sinano.ac.cn; Fax: +86-512-62872539; Tel: +86-512-62872539
[b]Academy for Advanced Interdisciplinary Studies, Peking University, Beijing, 100871, China
[c]Department of Biological Sciences, Xi'an Jiaotong-Liverpool University, Suzhou, 215123, China
[d]Institute for Viral Disease Control and Prevention, Chinese Center for Disease Control and Prevention, Beijing, 102206, China
[e]Institute of Biophysics, Chinese Academy of Sciences, Beijing, 100101, China
[f]Graduate University of the Chinese Academy of Sciences, Beijing, 100049, China

† Electronic Supplementary Information (ESI) available: See DOI: 10.1039/c2jm16572d

adjusting the buffer properties of protein solutions, one has very few choices in modifying the surface properties of micro-well plates, which are typically made from polystyrene. But for protein microarrays, each spot consumes only several nL of protein solution. Such small volumes of protein solution are very sensitive to the surface properties of SSM and environmental conditions. However, the surface chemistry of polymer coated iPDMS (shortened as iPDMS hereafter) could be finely tuned. Thus, it is possible for us to conduct a systematic study on the detailed process of protein microarray fabrication and assay.

In this paper, we first inspected the interactions between the iPDMS surface, proteins, reagents and environment throughout the entire protein microarray process. Next, we discussed their impacts on the quality of microarray. Then, we identified the elements leading to array defects (exosmosis, coffee ring and overflow) and corresponding strategies to avoid them. Through this research, we summarized the optimal parameters and conditions for protein microarray fabrication based on iPDMS sheets. We also identified some universal fundamental characteristics of protein microarray fabrication, which may benefit other SSM.

Experimental

Preparation and surface characterization of iPDMS sheets

Details of the iPDMS preparation can be found in a previous publication.[36] (1) **Surface Profiler.** An Alpha-Step IQ surface profiler (KLA Tencor, US) was used to characterize the thickness of the polymer membranes on the iPDMS surface. Before immersion in the surface initiated polymerization (SIP) reaction solution, half of the iPDMS surface was firmly covered with a silicon wafer so that the solution could not infiltrate and the initiator at the iPDMS surface could not initiate SIP. After the SIP reaction, the silicon wafer was removed. Before the surface profiling, a 10 nm thickness of gold was sputter-coated on the surface of the partially modified iPDMS to cushion the elasticity, so that the experiment could be more reliably performed. The surface profiler tip moved over the boundary of the iPDMS and polymeric film and reported a step height difference, which was the thickness of the polymeric film. **(2) Surface Tension.** The surface tension of all the buffer solutions and array protein solutions were measured by a Dataphysics DCAT2120 tensiometer equipped with a Wilhelmy plate at room temperature. The critical surface tension of the iPDMS sheets was measured according Zisman's method.[37] First, on the surface of the iPDMS sheet the contact angles of double distilled water, glycerol, and formamide, which have known surface tensions, were measured. Then, the critical surface tension was calculated using the SCA31 software (Dataphysics, Germany). See the ESI† for other surface characterization.

Protein microarray fabrication and ELISA

Details of the protein microarray preparation and ELISA processing can be found in a previous publication.[33] A Roche Diagnostics Elecsys 2010 system (Roche, USA) was used to calibrate the specific tumor marker concentration in human serum samples. All the serums were directly analyzed without any pretreatments.

Results and discussion

We divided the entire protein microarray experiment to two major stages: fabrication and assay. The fabrication process typically lasted for 24 h and was further divided into a contacting subprocess (step 1, from time 0 to ~1 h) and a fixing subprocess (step 2, from 1 to 24 h, Scheme 1a). The contacting subprocess began with the operation of arraying several nanoliters of protein solution onto the SSM. Spreading out of the array spots was immediately observed, as well as the evaporation of water from the array spots. Glycerol in the array protein solution slowed down the evaporation of water, which was the key to the success of the fixing subprocess. There was no clear demarkation between the contacting and fixing subprocess; however, we believe that the array spots reached a relatively steady state after 1 h. For the remaining 23 h, the capture antibodies were chemically or physically bonded onto the surface of iPDMS. Our results (data not shown) indicated that shortening the fixing process from 23 h to 6 h reduces the final signal of assay, while

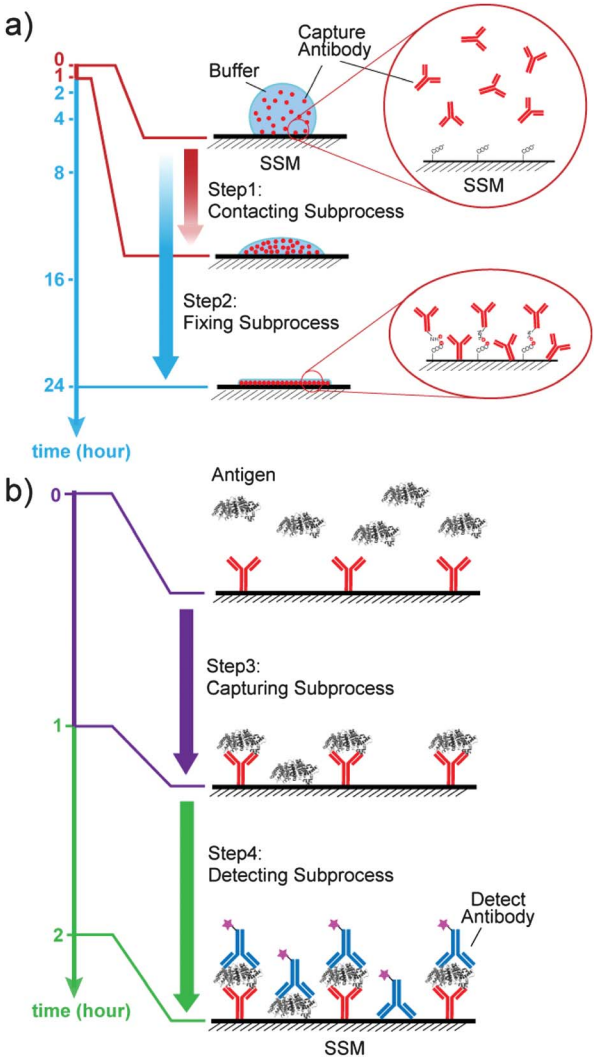

Scheme 1 Illustration of the entire protein microarray process. a) Two main subprocesses and dominant interactions during the fabrication stage. b) Two main subprocesses and interactions during the assay stage.

there was no improvement in signal when extending the fixing process to 48 h. Thus, the optimal time duration was 24 h for the fabrication stage.

Using the sandwich protocol as an example, the assay stage was composed of two subprocesses, with 1 h for each. In the capturing subprocess (step 3), the target proteins in serum (or specimen) specifically bond to the immobilized capture antibodies. In the detecting subprocess (step 4), the detection antibodies specifically bond to the target proteins, which have been captured by the immobilized capture antibodies (Scheme 1b). NPA could occur in both steps as indicated in Scheme 1b and was the main source of noise in ELISA. We demonstrated previously that iPDMS has intrinsic anti-NPA properties and could reduce NPA noise to a level below the detection limit of instruments, thus allowing us to achieve high sensitivity using higher amplification power.[33,38] We thereafter focused on the optimization of the fabrication stage.

We identified the following factors that play a role in the fabrication stage: (1) the critical surface tension of iPDMS, (2) surface tension of the array protein solution, (3) the concentration of capture antibody ([capture antibody], *i.e.*, the array protein solution), (4) the volume of each drop of array protein solution (shortened as array volume thereafter), and (5) environmental conditions.

The critical surface tension of iPDMS

We tuned the critical surface tension of iPDMS by adjusting the duration of SIP, which is difficult to do for other SSM such as polystyrene well plates or NC. Details of the preparation of iPDMS and SIP can be found in previous publications.[36] It was difficult to measure the thickness of resulting polymer coating by ellipsometry because iPDMS is a transparent material. To overcome this characterization problem, we prepared partially modified iPDMS samples as outlined in Fig. 1a and obtained thickness information *via* a surface profiling experiment. Fig. 1b presents the SEM results of this partially modified iPDMS sheet, on which one can easily distinguish the area covered with (left half) and without poly(OEGMA) (see Fig. S1, ESI† for more SEM results). We found that the thickness of the poly(OEGMA) layer correlated with the SIP time, and negatively correlated with the contact angle (Fig. 1c), which was attributed to the development of wrinkling.[39]. Contact angles were based on double distilled water unless otherwise stated. Thus, we could tune the critical surface tension of iPDMS sheets by adjusting the SIP duration. The surface modification was further confirmed by the XPS results (Fig. S2, ESI†).

With the ability to tune the critical surface tension of iPDMS, we were now able to study how the SSM impacts the quality and performance of protein microarrays, and then some optimization strategies were proposed.

Occurrence and avoidance of array defects

Successful fabrication is the premise for a good protein microarray. Only faultless arraying and effective fixing can ensure a microarray with an orderly array, universal spot size and a sufficient amount of fixed capture antibodies.[15] Excluding instrumental elements, array defects are the most common

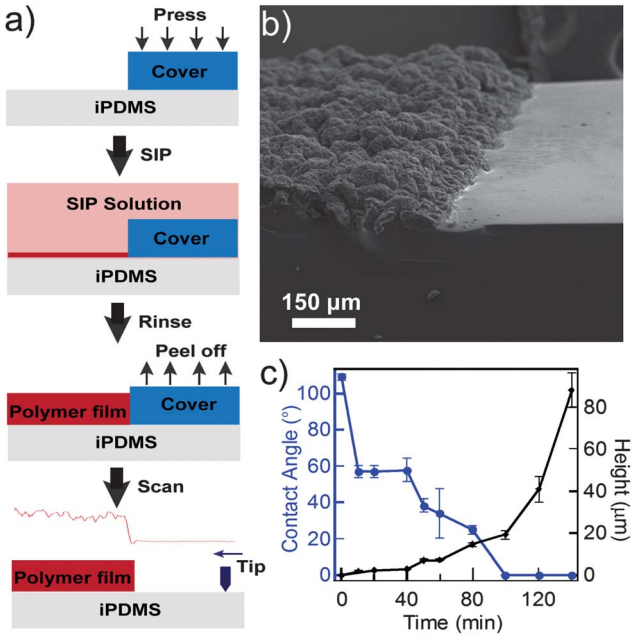

Fig. 1 Surface characterization of poly(OEGMA) coated iPDMS. (a) Schematic illustration of the surface profiling experiments that were designed for height, morphology and surface chemistry characterization of iPDMS after SIP. (b) SEM of a cross section view of partially modified iPDMS. See text for a detailed discussion. (c) Height determination by the surface profiler (black) and contact angle (blue) were plotted against SIP time.

problems that must be avoided throughout the fabrication stage. Additionally, for a 2D or wrinkled microarray substrate, the most common array defects are exosmosis,[40–42] hollow spaces (coffee ring)[30,35,43] and overflow.[14,44,45]

Formation of the exosmosis defect is shown in Fig. 2a. It generally occurred at the very beginning when each drop of protein solution was arrayed onto the SSM. The array protein solution drop wets the surface very quickly because the surface tension of the protein solution was much smaller than the critical surface tension of the SSM.[37] An exosmosis defect can cause array spots to overspread and have an irregular shape, as well as cause adjacent spots to mix together (Fig. S3a, ESI†). Exosmosis can also lead to a very low signal. To avoid exosmosis, the surface tension of the protein solution should less than the critical surface tension of the SSM.[37] However, we found that protein solutions with different pH values or protein concentrations had similar surface tensions of around 30 mN m^{-1} (Table S1, ESI†). Thus, the only option was to adjust the critical surface tension of the SSM to avoid exosmosis. In this case it was performed by surface modification of iPDMS *via* SIP. The results indicated that the critical surface tension of iPDMS sheets had a perfect linear relationship with their contact angle, which was consistent with Zisman's theory[37] (Fig. 2b). For most buffers and protein solutions the exosmosis defect could be avoided when the contact angle of the iPDMS sheets was greater than 50° and the critical surface tension was below ~50 mN m^{-1} (Fig. S3d, ESI†). In summary, all iPDMS sheets used in the following experiments were prepared with 40 min of SIP time, resulting an iPDMS sheet with a ~10 μm poly(OEGMA) layer, which had a contact angle over 50°.

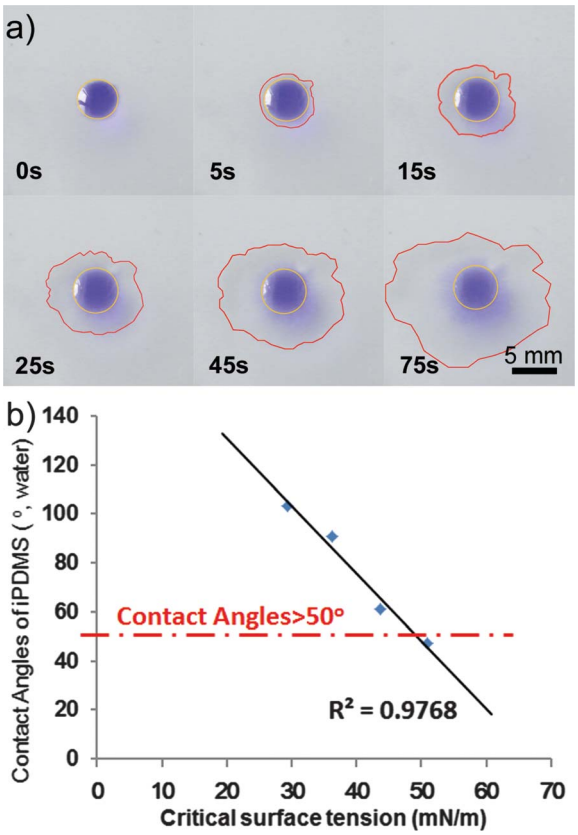

Fig. 2 a) The formation of the exosmosis defect (the exosmosis area was illustrated with red curves). b) The linear relationship between the contact angle and critical surface tension of iPDMS films. The dashed line indicates the lower limit of the iPDMS surface, contact angle = 50°, which can prevent the exosmosis defect.

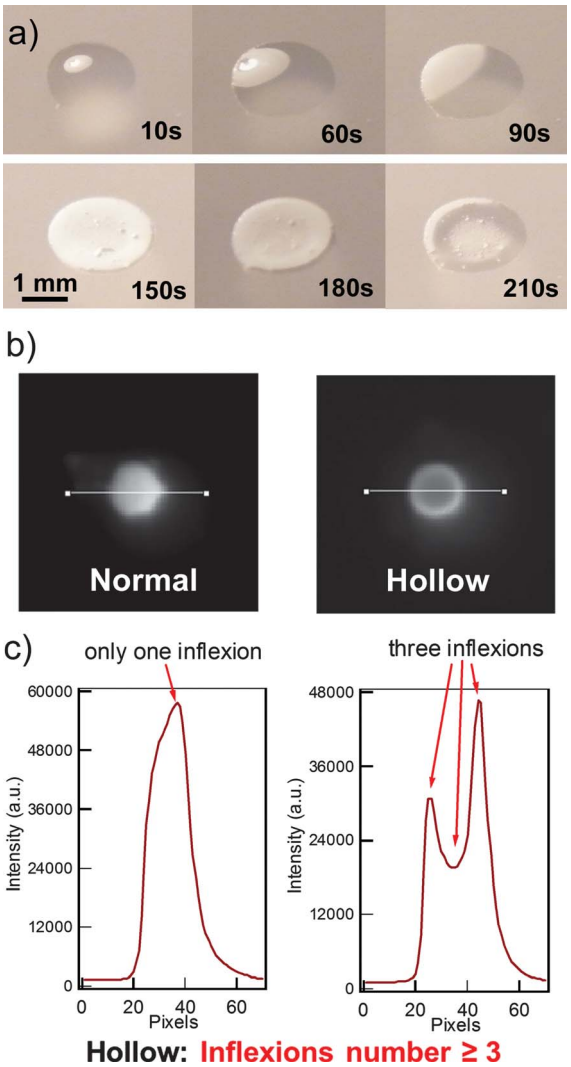

Fig. 3 a) The formation process of the coffee ring. b) Comparison of the normal signal spot and the hollow spaces signal spot. c) The signal line profile signal across a normal spot and coffee ring.

The hollow spaces defect (referred to as the coffee ring thereafter) also occurs during the fabrication stage (Fig. 3a). Deegan *et.al.*,[46] studied the forming process of this defect, and demonstrated that when the evaporation of spot solvent is much faster than the spot edge shrinkage, the solute would accumulate at the spot edge, and form a coffee ring. In the chemiluminescent image, a signal spot with a coffee ring can usually be detected by a higher signal of the spot edge than that of the center, which is in contrast to a normal spot (Fig. 3b). As Fig. 3b–3c show, we introduced a signal profile curve to define the coffee ring. We drew a straight line through the center of the spot. Each pixel on this line had a sequence number and a signal value (depending on the grey scale of the pixel). Then we were able to obtain a signal profile curve with the signal value as the vertical coordinate and the sequence number as the horizontal coordinate. If the curve of a signal spot had three or more inflexions, we defined this spot as having a coffee ring; otherwise the spot was defined as normal if it had one or two inflexions.

The formation of the coffee ring is determined by the balance between solvent evaporation and spot edge shrinkage. For protein microarray fabrication, because the array protein solutions have a constant surface tension value of about 30 mN m^{-1}, the forming process of coffee ring is mainly influenced by the hydrophobility of the SSM, array volume, the temperature and the humidity of the fixing process. As shown in Fig. 4a, under specific conditions (*i.e.*, 40 °C and 40% humidity), the iPDMS sheets with higher contact angles led to smaller spot diameters and then weaken the formation of coffee ring. On the other hand, when the other factors remained unchanged, higher environmental temperatures resulted in faster solvent evaporation, which is advantageous to coffee ring formation. However, higher humidity could slow the evaporation process and weaken coffee ring formation. Finally, within one iPDMS sheet, the array volume was positively related to the spot diameter (Fig. 4b, more detailed data are shown in Fig. S4, ESI†). Therefore, a smaller array volume meant smaller spot diameter, which can also prevent the coffee ring forming. In conclusion, when the contact angle of iPDMS sheets was greater than 50°, and the array volume was below 10 nL, the resulting spots had a diameter no bigger than 0.58 ± 0.02 mm. When fixed under 25 °C and 60% humidity, the formation of the coffee ring defect could be prevented. (Fig. 4c)

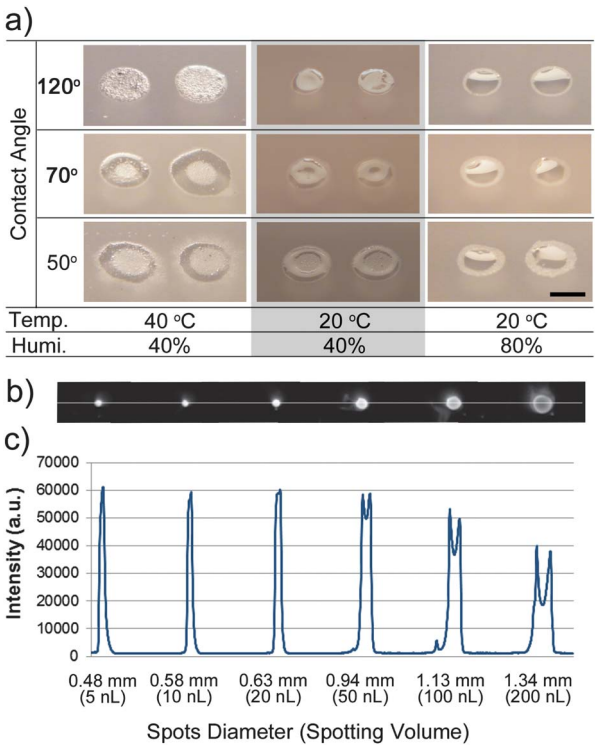

Fig. 4 Influencing factors of the coffee ring formation. a) The influence of contact angle (surface tension), temperature and humidity (all spots had the same original volume of 1 μL, the scale bar represents 1 mm). Chemiluminesence result image (b), and signal profile results (c) of array spots with different spotting volume (spots diameter). The results of b), c) were obtained from an iPDMS SSM with a contact angle of 75°, and fixed at 25 °C, 60% humidity.

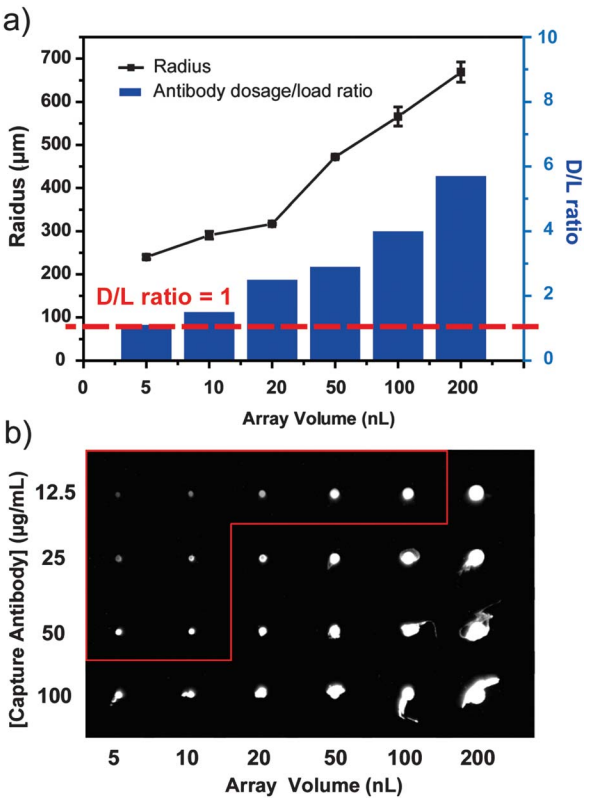

Fig. 5 a) The different spotting radii and antibody dosage/load (D/L) ratios of various array volumes. The black line shows the relationship between array volume and spot radius ($n = 24$). The blue histogram shows the D/L ratio, D: number of antibodies in different array volumes ([capture antibody] = 50 μg mL^{-1}), L: number of antibodies that different spotting diameters can arrange. b) The chemiluminescence results of different array volumes with various [capture antibody]. The red line defined the no-overflow region.

Unlike exosmosis, overflow defects can be observed only in the final chemiluminescent detection assay of a protein microarray. Compared with normal round signal spots, the overflow defect presents as spots with irregular trailing or glowing. We supposed these redundant trailings come from the overload of capture antibodies. One drop of array protein solution forms an array spot within a certain area. However, only a certain amount of capture antibodies can be fixed in this area. If the array protein solution drop contains too many capture antibodies to be fixed, those excess antibodies would flow out and irregularly absorb on SSM that surrounds the spot area. We verified this hypothesis in two ways.

Firstly, we roughly counted the numbers of capture antibody molecules that were contained in a drop of array protein solution (IgG, 50 μg mL^{-1}) with different array volumes (shortened as D hereafter). We measured the average spot radius that these array protein solution drops (with each array volume) formed on an iPDMS sheet (Fig. 5a, black line). Then, we estimated the numbers of capture antibodies could be fixed in each spot's area (the iPDMS sheet surface was approximated as a flat surface) in a compact arranged pattern (shortened as L thereafter). The D/L ratio showed that under a capture antibody concentration of 50 μg mL^{-1}, when the array volume was greater than 10 nL, the capture antibodies number that a drop of array solution contained were in far more excess than a corresponding array spot area could arrange in a compact pattern (Fig. 5a, blue histogram, D/L ratio >1), thus lead to the overflow defect.

Secondly, we designed a confirmatory experiment. A 4 × 6 array of goat IgG was arrayed onto an iPDMS sheet (contact angle = 75°). As seen in Fig. 5b, the spots in a vertical line had the same array volume and the spots in a horizontal row had the same capture concentration in the array protein solution. This assay was carried out following the direct ELISA protocol. For a solution of 50 μg mL^{-1}, we found that only the spots with 5 or 10 nL array volumes did not experience any overflow, which was in perfect agreement with our calculation in Fig. 5a. Furthermore, abiding by the D/L ratio = 1 principle (Fig. 5a, red dash line), we defined a "no overflow" region in Fig. 5b (area defined by the red line), which further demonstrated that the overflow defect does come from the unfixed capture antibodies. In addition, we found that the overflow defect easily occurred on iPDMS sheets with a contact angle over 90°, since high contact angle resulted in smaller array spots and less capture antibody loading capacity (about 20% reduction, data not shown).

Active loaded capture antibodies

During the research of overflow avoidance, we obtained preliminary knowledge of the loading capacity of iPDMS

sheets: about 50 μg mL^{-1} IgG for an array volume of 10 nL under an optimal contact angle range (50° < contact angle < 90°). We further compared the loading capacity of iPDMS sheets and NC films (Millipore, USA). Microarrays were fabricated on both iPDMS sheets and NC films in the same pattern. Each pattern contained 24 array spots (10 nL/spot) of capture antibody (IgG, 0.2–400 μg mL^{-1}, two spots per gradient). Then, detection solutions with various concentration of detection antibody (anti-IgG, 50–4000 ng mL^{-1}) were added into each of the different microarrays. All the experimental conditions were kept the same, except the NC films required a blocking process and more powerful rinsing.

Under the same conditions, iPDMS was more prone to the overflow problem, indicating that the NC film had a higher loading capacity. However, a more complex pattern was found for the signal as a function of loading [capture antibody] for iPDMS and NC. In general, the signal increased as [capture antibody] increased on both kinds of SSM. On the iPDMS sheets, the signal reached a saturation value when [capture antibody] reached 50 μg mL^{-1}, which was in agreement with the fact that 50 μg mL^{-1} was the theoretical maximum loading concentration (Fig. 5). On the NC film, the signal reached a saturation value when [capture antibody] reached 400 μg mL^{-1}, indicating NC had a higher loading capacity. The most intriguing results came from the signal ratio (S_{iPDMS}/S_{NC}) chart of the two SSMs (Fig. 6a).

For [capture antibody] from 0.2–5 μg mL^{-1}, iPDMS sheets and NC films gave similar signal (S_{iPDMS}/S_{NC} ~1). As the [capture antibody] continue to increase, S_{iPDMS}/S_{NC} became >1 and reached its maximum at 8 when the [capture antibody] was about 25 μg mL^{-1}. The ratio decreased to about 2 again after the concentration was greater than 400 μg mL^{-1}. This trend was attributed to the wrinkled and 3D nature of iPDMS sheets and NC films, respectively. As shown in Fig. 1 and Fig. S1, ESI,† iPDMS sheets have a wrinkled surface with micron scale wrinkles that are composed of poly(OEGMA) brushes.[39,47,48] While this wrinkled surface has a higher loading capacity than a planar surface, most of the fixed capture antibodies were still accessible to give effective signals. On the other hand, although the NC film, as a porous film with a 3D network structure, has a higher loading capacity[33] than iPDMS, the porous structure would inevitably pose difficulties for the detecting antibody to access immobilized capture antibodies. As a result, on NC film, 2–4 times more capture antibodies are needed for an equal signal with iPDMS sheets for [capture antibody] at 5–400 μg mL^{-1}. When the [capture antibody] is less than 5 μg mL^{-1}, the total capture antibody amount is too small to show an obvious signal difference between the two SSM; and when the [capture antibody] is greater than 400 μg mL^{-1}, there are excess capture antibodies to give effective signals on the spot region of NC film surface. Furthermore, such porous structure may cause nonspecific trapping of detecting antibodies, therefore requiring tedious washing operations.

Based on the above results, we further explored the optimal [capture antibody] of five tumor markers on iPDMS sheets and NC films. From the data in Table 1, we can see that the optimal capture antibody on NC film (C_{NC}) was generally five

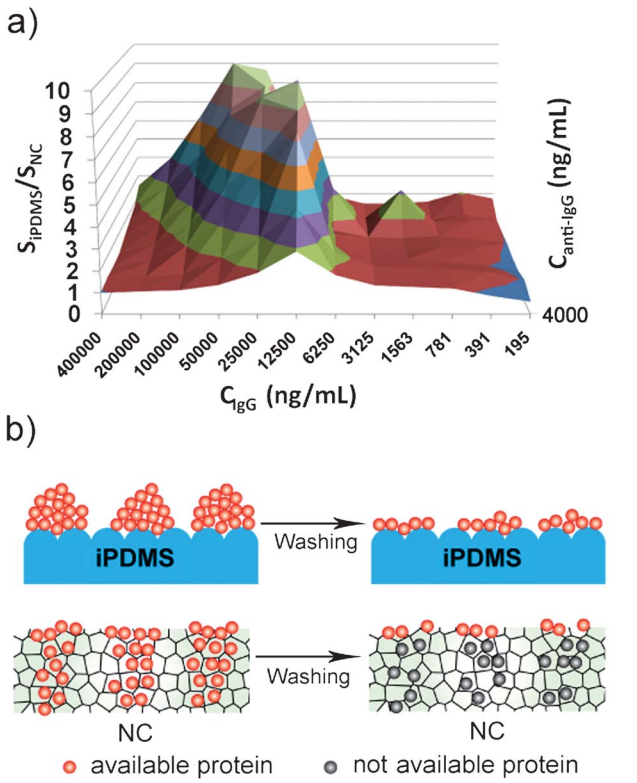

Fig. 6 Active loaded capture antibodies. a) The signal ratio of iPDMS/NC under different conditions. C_{IgG} and $C_{anti-IgG}$ are the concentrations of capture IgG and detection anti-IgG, respectively; S_{iPDMS}/S_{NC} is the signal ratio of these two SSM. b) The 3D nature of NC film caused some of the loaded capture antibodies to be inaccessible.

times higher or more than on iPDMS (C_{iPDMS}) sheets for the same kind of tumor marker. When the [capture antibody] was fixed at 0.1 mg mL^{-1}, and other conditions were unchanged, the signal ratio of each tumor marker on iPDMS sheets to NC films is shown as S_{iPDMS}/S_{NC} in Table 1. For AFP and three other markers, 0.1 m g mL^{-1} was very close to the C_{iPDMS}, but was too small for C_{NC}, which resulted in much higher signal on iPDMS sheets. On the contrary, for CA19-9, this concentration was beyond the C_{iPDMS} and very close to the C_{NC}, so a similar signal was obtained on both SSM. In conclusion, a 3D network structure and large specific surface area are not the necessary properties for an excellent protein microarray SSM. The iPDMS sheets, with appropriate loading capacity, can greatly save and effectively utilize the precious protein resources.

We further demonstrated that protein microarrays based on iPDMS after optimization were comparable with the Roch Diagnostics Elecsys 2010 system (single index assay). Five tumor markers (CA199, CA125, CEA, AFP or CK19) of 25 serum samples were measured by the Roche Method as well as protein microarrays based on iPDMS and NC. The results showed that the linear correlation coefficient of 0.98 between the Roche and the iPDMS (Fig. S5a, ESI†) far outclassed the coefficient of 0.89 between the Roche and the NC (Fig. S5b, ESI†), indicating that the protein microarray based on the iPDMS sheet had excellent low-end sensitivity.

Table 1 Multiplexed ELISAs on both iPDMS and NC under the same conditions

	AFP	CEA	CK19	SCC	CA19-9
$C_{\text{Capture Ab}}$ (mg mL^{-1})	0.1	0.1	0.1	0.1	0.1
C_{iPDMS}[a] (mg mL^{-1})	0.08	0.08	0.1	0.1	0.04
C_{NC}[b] (mg mL^{-1})	0.5	0.6	0.8	0.5	0.2
C_{antigen}	124.1 ng mL^{-1}	49.5 ng mL^{-1}	27 ng mL^{-1}	21.6 ng mL^{-1}	174.1 U mL^{-1}
$C_{\text{Detection Ab}}$ (μg mL^{-1})	0.11	0.04	0.16	0.5	0.4
$S_{\text{iPDMS}}/S_{\text{NC}}$	**7.5**	**5.0**	**4.7**	**3.0**	**0.8**

[a] C_{iPDMS} is the optimized spot concentration of each biomarkers on iPDMS sheets. [b] C_{NC} is the optimized spot concentration of each biomarkers on NC films.

Conclusions

In summary, given the tunability of iPDMS surface chemistry, we defined the optimized protein microarray fabricating conditions on iPDMS sheets: 50° < contact angle < 90°, array volume ≤10 nL, [capture antibody] at 50 μg mL^{-1}, fixed at 25 °C, and 60% humidity. We also demonstrated that, as a substrate of protein microarray, the iPDMS sheet possessed an appropriate surface morphology. The studies on the origins of array defects (exosmosis, coffee ring and overflow) may find use in protein microarray fabrication on other SSM. After optimization, both the dynamic range and low-end sensitivity of the iPDMS multiplex protein microarray were improved by about four orders of magnitude and deceased to about 10 pg mL^{-1} (*i.e.*, 0.1 fM), respectively. With improved performance, protein microarray will find more applications in proteomics, drug discovery and disease diagnosis.

Acknowledgements

This work was supported by the 100 Talents Program of CAS (08BM031001), the National Basic Research Program of China (2009CB320300) and the NSFC (21074148) to H.M. We thank the Public Center for Characterization and Test at SINANO for the SEM support, Dr X. L. Yang and Mr H. K. Xu for providing the serum samples, Professor Jinglin Xie for the help with XPS.

References

1 K. Büssow, D. Cahill, W. Nietfeld, D. Bancroft, E. Scherzinger, H. Lehrach and G. Walter, *Nucleic Acids Res.*, 1998, **26**, 5007–5008.
2 G. MacBeath, A. N. Koehler and S. L. Schreiber, *J. Am. Chem. Soc.*, 1999, **121**, 7967–7968.
3 R. M. T. de Wildt, C. R. Mundy, B. D. Gorick and I. M. Tomlinson, *Nat. Biotechnol.*, 2000, **18**, 989–994.
4 H. Zhu, J. F. Klemic, S. Chang, P. Bertone, A. Casamayor, K. G. Klemic, D. Smith, M. Gerstein, M. A. Reed and M. Snyder, *Nat. Genet.*, 2000, **26**, 283–289.
5 B. T. Houseman, J. H. Huh, S. J. Kron and M. Mrksich, *Nat. Biotechnol.*, 2002, **20**, 270–274.
6 S. Lemeer, R. Ruijtenbeek, M. W. H. Pinkse, C. Jopling, A. J. R. Heck, J. den Hertog and M. Slijper, *Mol. Cell. Proteomics*, 2007, **6**, 2088–2099.
7 E. Murray, E. O. McKenna, L. R. Burch, J. Dillon, P. Langridge-Smith, W. Kolch, A. Pitt and T. R. Hupp, *Biochemistry*, 2007, **46**, 13742–13751.
8 J. Gao, D. Liu and Z. Wang, *Anal. Chem.*, 2008, **80**, 8822–8827.
9 J. D. McBride, F. G. Gabriel, J. Fordham, T. Kolind, G. Barcenas-Morales, D. A. Isenberg, M. Swana, P. J. Delves, T. Lund, I. A. Cree and I. M. Roitt, *Clin. Chem.*, 2008, **54**, 883–890.
10 T. R. Northen, M. P. Greving and N. W. Woodbury, *Adv. Mater.*, 2008, **20**, 4691–4697.
11 M. W. Foster, M. T. Forrester and J. S. Stamler, *Proc. Natl. Acad. Sci. U. S. A.*, 2009, **106**, 18948–18953.
12 H. Rodriguez, Z. Tezak, M. Mesri, S. A. Carr, D. C. Liebler, S. J. Fisher, P. Tempst, T. Hiltke, L. G. Kessler, C. R. Kinsinger, R. Philip, D. F. Ransohoff, S. J. Skates, F. E. Regnier and N. L. Anderson, E. Mansfield and on behalf of the Workshop Participants, *Clin. Chem.*, 2009, **56**, 237–243.
13 H. Wu, J. Ge and S. Q. Yao, *Angew. Chem.*, 2010, **122**, 6678–6682.
14 X. Zhou and J. Zhou, *Proteomics*, 2006, **6**, 1415–1426.
15 A. A. Ellington, I. J. Kullo, K. R. Bailey and G. G. Klee, *Clin. Chem.*, 2009, **56**, 186–193.
16 D. J. Cahill, *J. Immunol. Methods*, 2001, **250**, 81–91.
17 L. J. Holt, C. Enever, R. M. T. de Wildt and I. M. Tomlinson, *Curr. Opin. Biotechnol.*, 2000, **11**, 445–449.
18 H. Ge, *Nucleic Acids Res.*, 2000, **28**, 3e.
19 J. Hanes, C. Schaffitzel, A. Knappik and A. Pluckthun, *Nat. Biotechnol.*, 2000, **18**, 1287–1292.
20 K. Nord, E. Gunneriusson, M. Uhlén and P.-Å. Nygren, *J. Biotechnol.*, 2000, **80**, 45–54.
21 P. Lohse and M. Wright, *Curr. Opin. Drug Disc.*, 2001, **4**, 198–204.
22 B. Schweitzer, S. Roberts, B. Grimwade, W. Shao, M. Wang, Q. Fu, Q. Shu, I. Laroche, Z. Zhou, V. T. Tchernev, J. Christiansen, M. Velleca and S. F. Kingsmore, *Nat. Biotechnol.*, 2002, **20**, 359–365.
23 Z. Chen, S. M. Tabakman, A. P. Goodwin, M. G. Kattah, D. Daranciang, X. Wang, G. Zhang, X. Li, Z. Liu, P. J. Utz, K. Jiang, S. Fan and H. Dai, *Nat. Biotechnol.*, 2008, **26**, 1285–1292.
24 C.-C. You, O. R. Miranda, B. Gider, P. S. Ghosh, I.-B. Kim, B. Erdogan, S. A. Krovi, U. H. F. Bunz and V. M. Rotello, *Nat. Nanotechnol.*, 2007, **2**, 318–323.
25 H. D. Sikes, R. Jenison and C. N. Bowman, *Lab Chip*, 2009, **9**, 653–656.
26 O. R. Miranda, C.-C. You, R. Phillips, I.-B. Kim, P. S. Ghosh, U. H. F. Bunz and V. M. Rotello, *J. Am. Chem. Soc.*, 2007, **129**, 9856–9857.
27 J. Dai, G. L. Baker and M. L. Bruening, *Anal. Chem.*, 2006, **78**, 135–140.
28 A. Ressine, S. Ekström, G. Marko-Varga and T. Laurell, *Anal. Chem.*, 2003, **75**, 6968–6974.
29 P. Angenendt, J. Glökler, D. Murphy, H. Lehrach and D. J. Cahill, *Anal. Chem.*, 2002, **309**, 253–260.
30 V. Afanassiev, V. Hanemann and S. Wölfl, *Nucleic Acids Res.*, 2000, **28**, 66e.
31 D. W. Grainger, C. H. Greef, P. Gong and Lochhead, *J. Mol. Biol.*, 2007, **381**, 37–57.
32 P. Wu, D. G. Castner and D. W. Grainger, *J. Biomater. Sci., Polym. Ed.*, 2008, **19**, 725–753.
33 H. Ma, Y. Wu, X. Yang, X. Liu, J. He, L. Fu, J. Wang, H. Xu, Y. Shi and R. Zhong, *Anal. Chem.*, 2010, **82**, 6338–6342.
34 J. J. Gray, *Curr. Opin. Struct. Biol.*, 2004, **14**, 110–115.
35 J. Camarero and Y. Kwon, *Int. J. Pept. Res. Ther.*, 2008, **14**, 351–357.
36 Y. Z. Wu, Y. Y. Huang and H. W. Ma, *J. Am. Chem. Soc.*, 2007, **129**, 7226–7227.
37 A. H. Ellison, H. W. Fox and W. A. Zisman, *J. Phys. Chem.*, 1953, **57**, 622–627.
38 H. W. Ma, M. Wells, T. P. Beebe and A. Chilkoti, *Adv. Funct. Mater.*, 2006, **16**, 640–648.
39 Z. Li, S. Zhang, P. Zhang, D. Yang, G. Jin and H. Ma, *Polym. Adv. Technol.*, 2011.
40 R.-P. Huang, *J. Immunol. Methods*, 2001, **255**, 1–13.

41 P. Saviranta, R. Okon, A. Brinker, M. Warashina, J. Eppinger and B. H. Geierstanger, *Clin. Chem.*, 2004, **50**, 1907–1920.
42 I. Sielaff, A. Arnold, G. Godin, S. Tugulu, H.-A. Klok and K. Johnsson, *Chem. Bio. Chem.*, 2006, **7**, 194–202.
43 W. G. T. Willats, S. E. Rasmussen, T. Kristensen, J. D. Mikkelsen and J. P. Knox, *Proteomics*, 2002, **2**, 1666–1671.
44 Y. Liu, C. M. Li, W. Hu and Z. Lu, *Talanta*, 2009, **77**, 1165–1171.
45 P. Angenendt, J. Glökler, J. Sobek, H. Lehrach and D. J. Cahill, *J. Chromatogr., A*, 2003, **1009**, 97–104.
46 R. D. Deegan, O. Bakajin, T. F. Dupont, G. Huber, S. R. Nagel and T. A. Witten, *Nature*, 1997, **389**, 827–829.
47 Z. Li, D. Yang, X. Liu and H. Ma, *Macromol. Rapid Commun.*, 2009, **30**, 1549–1553.
48 P. Zhang, D. Yang, Z. Li and H. Ma, *Soft Matter*, 2010, **6**, 4580–4584.

